Engineering Structures 306 (2024) 117856

Contents lists available at ScienceDirect

Engineering Structures

journal homepage: www.elsevier.com/locate/engstruct

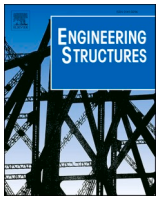

A novel analytical formulation for the stiffness of the component column web panel in shear with additional plates in bolted steel joints.

Manuel Lopez *, Alfonso Loureiro, Ruth Gutierrez, Jose M. Reinosa

University of A Coruña, Structural Analysis Laboratory, CITENI, Ferrol Industrial Campus, Mendizabal s/n Campus de Esteiro, 15403 Ferrol, Spain

ARTICLE INFO

Keywords:
Experimental
Finite element modelling
Components method
Column shear panel
Additional plates
Beam to column joint

ABSTRACT

Given that the stiffness of joints has an important influence on the global behavior of steel structures, considerable efforts have been made to develop methods to characterize their behavior. In the component method, that is adopted by Eurocode 3, one of the most relevant components is the column web panel in shear; however, this component has never been the subject of research when additional plates are welded between the column flanges to attach the secondary beams to the minor axis of the column. This paper proposes a stiffness formulation for the component column web panel in shear with additional plates, taking into account the stiffening contribution of these additional plates. To archive this, four experimental tests of beam-to-column joints were carried out, a finite element model was calibrated with the experimental data by comparing moment-rotation and moment-deformation curves, a parametric study of sixty different configurations was performed with the calibrated finite element models to obtain the stiffness of the component column web panel in shear and the initial stiffness of the joint. Then, the proposed stiffness formulation for the component was validated with the results of the parametric study, obtaining a very good agreement. Finally, a compilation of the stiffness formulation of all the components of the joint type extended end plate with additional plates was made and validated, when comparing this analytical stiffness with the initial stiffness of the joints of the parametric study, satisfactory concordance was found.

1. Introduction

Considering that joints play an important role in the behavior of steel structures, researchers have spent a lot of time and resources to characterize them, developing useful calculation methods and design codes. Faella et al. [1] and more recently Celik and Sakar [2] compiled different methodologies that have been developed, such as experimental, numerical, empirical, analytical, informational, or mechanical models. The component method is one of the best-known mechanical models that is also used in Eurocode 3 [3]. This method represents the joint by a combination of flexible components characterized by their stiffness and resistance, and has been widely used in beam-to-column configurations [1,4–6], but also in beam-to-beam joints [7,8].

For 2D joint configurations most of the components have been characterized; however, components for 3D joints have been less studied and are not recorded in most common design codes. De Lima et al. [9] and Costa et al. [10] studied the most common configuration, where the minor axis is attached directly to the web of the column. However, a useful 3D joint configuration exists when the secondary beams are attached to the minor axis of the column by additional plates welded between column flanges. This configuration presents several advantages over the most typical 3D joint, where the end plate of the secondary beam is attached directly to the column web. The most outstanding advantages are the absence of inference of the minor and major axis in the assembly stage and the increase of the column's stiffness. Several authors have performed tests and carried out studies about this typology. Cabrero et al. [10] have studied a joint where the additional plates were divided into top and bottom to attach the secondary beams, which also have a top and bottom end plate, on the minor axis. The additional and the end plates were attached by 4 bolts. In addition, Loureiro et al. [12] have studied the E-stub component that appears in the column of the joint configuration represented in Fig. 1.

The presence of these additional plates modifies the components of the column; therefore, the formulation of the components should be modified to take into account the effect of these additional plates. The affected components are the column flange in bending, the column web in tension, the column web in compression and the column web panel in shear. Cabrero et al. [10] and Loureiro et al. [12] have proposed

* Corresponding author.
E-mail address: manuel.lopez.lopez@udc.es (M. Lopez).

https://doi.org/10.1016/j.engstruct.2024.117856
Received 27 November 2023; Received in revised form 20 February 2024; Accepted 10 March 2024
Available online 16 March 2024

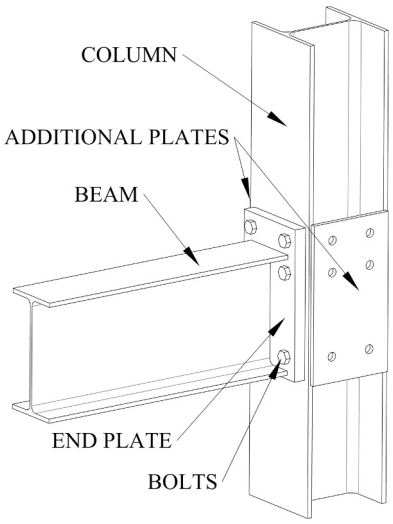

Fig. 1. Joint configuration.

analytical formulations for some of these components, but the column web panel in shear has so far not been studied.

The component, column web panel in shear, has special importance in the behavior of the joint, having been the subject of analysis in numerous studies over the last few years. Bayo et al. [13] dealt with the formulation of a cruciform finite element for three types of web panels. Corman et al. [14], based on the extensive use of finite element analysis, developed a new analytical model that provides a more coherent estimation of the plastic shear resistance of the panel zone, whose results outperform the existing models. Golea et al. [15] proposed an innovative mechanical model that incorporates the variation of the shear forces on the height of the column web panel. Lopez et al. [16] characterized the shear behavior of the trapezoidal column web panels in welded joints. Augusto et al. [17] proposed a practical and efficient methodology to extract the force-deformation behavior of the column web components from experimental tests and numerical simulations. However, there is no study or mechanical model that addresses the aforementioned case of the column web panel in shear with additional plates between the column flanges.

After identifying the novelty of the problem, this article uses a scientifically based methodology consisting of four basic steps: (i) development of an experimental campaign, (ii) development and validation of a finite element model, (iii) development of a comprehensive parametric study to highlight the key parameters influencing the column web panel in shear, (iv) development and validation of a formulation that encompasses the effect of the key parameters.

The aim of this article is to characterize the stiffness of the component column web panel in shear when additional plates are welded between the column flanges. This component appears in the joint configuration represented in Fig. 1. Thus, four experimental tests with different geometries were carried out and the moment-rotation and moment-deformation curves were obtained. Finite element models were made and calibrated with the results of the experimental campaign. The results of the finite element models were discussed to understand the effects of the additional plates on the joint behavior. An extensive parametric study with these calibrated finite element models was

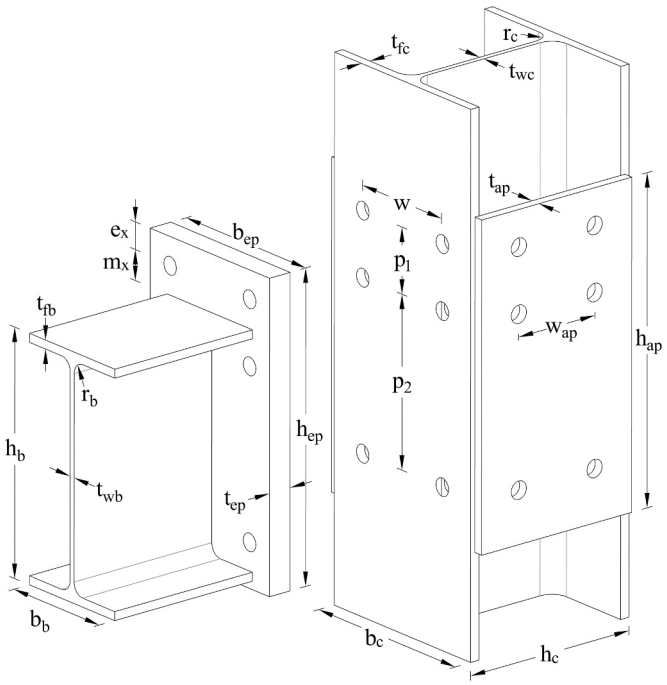

Fig. 2. Parameters of the joint.

developed, covering the most typical beam-to-column configurations, obtaining the stiffness of the component column web panel in shear and the initial stiffness of the joint. A novel stiffness formulation is proposed for the component column web panel in shear when additional plates are welded between column flanges. This formulation was validated by comparison with the stiffness of the finite element models of the parametric study. Finally, a compilation of the formulation of all the components involved in the mechanical model of the joint was made, based on different sources. The stiffness of this mechanical model was compared and validated with the initial stiffness of the joints of the parametric study.

2. Experimental program

The experimental program was designed with the objective to learn the influence of the additional plates in the stiffness of the joint. To do so, four beam-to-column joints with different configurations were tested. Table 1 shows, for each test, the type of profile for the beam and column, and the dimensions of the additional and the end plates (see Fig. 2). The nominal values of the additional plates' thickness (t_{ap}) were 8 mm for Test-1 and Test-3, 12 mm for Test-2 and 15 mm for Test-4. The height of the additional plate is h_{ap}. The horizontal distance between bolts is w, the distance between the first and second bolt row is p_1 and between the second and third row is p_2. The horizontal distance between bolt holes in the additional plates is w_{ap}. The width and height of the end plate are b_{ep} and h_{ep} respectively. The distance between the top part of the end plate and the first row is e_x and m_x from the first row to the top flange of beam. In all cases, the bolt type was 10.9TR20 in 22 mm diameter drilled holes. In order to reduce the influence in the stiffness of the joint and in the column web panel, the thickness of the end plate (t_{ep})

Table 1
Experimental configurations (dimensions in millimeters).

Test	Column	Beam	t_{ap}	h_{ap}	w	p_1	p_2	w_{ap}	b_{ep}	h_{ep}	t_{ep}	e_x	m_x	L_b
TEST-1	HEA 200	IPE 300	7.9	402	110	80	210	100	180	378	30	35	35	925
TEST-2	HEA 200	IPE 300	11.6	401	110	80	210	100	180	375	30	35	35	918
TEST-3	HEA 240	IPE 300	7.9	402	140	80	211	110	208	381	30	35	35	895
TEST-4	HEA 240	IPE 300	14.8	400	140	80	210	110	207	382	30	35	35	895

Table 2
Real dimensions of the columns (dimensions in millimeters).

Profile	t_{fc}	t_{wc}	h_c	b_c	r_c
HEA 200	9.4	6.8	191	200	18
HEA 240	11.9	7.9	235	240	21

Table 3
Real dimensions of the beam (dimensions in millimeters).

Profile	t_{fb}	t_{wb}	h_b	b_b	r_b
IPE 300	10.2	7.1	298	149	15

Table 4
Material properties.

Material	f_y (MPa)	E (GPa)	f_u (MPa)	ε_u
HEA 200	315	186.6	441	0.275
HEA 240	400	216.0	533	0.234
IPE 300	355	208.5	448	0.155
Plate 8 mm	377	201.6	470	0.243
Plate 12 mm	369	212.3	478	0.148
Plate 15 mm	342	209.9	465	0.196
Plate 30 mm	320	200.4	440	0.211

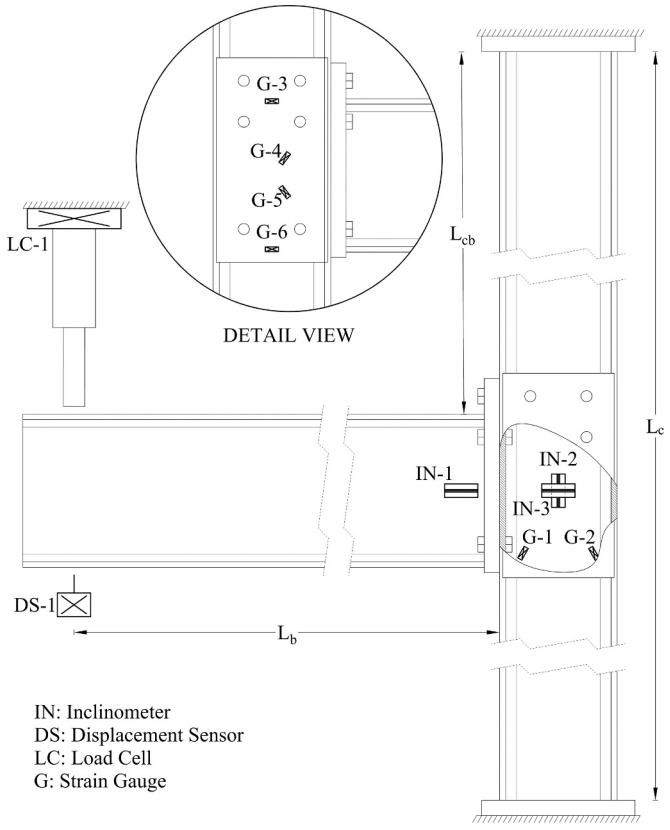

Fig. 3. Instrumentation of the tests. Break view in the left additional plate and detail view of the right additional plate.

was 30 mm in all tests. L_b is the distance from the point where load was applied to the column flange.

Table 2 and Table 3 show the real dimension of the column and beam profiles, respectively, obtained by the arithmetic mean of the measurement at several points. For the column profiles the parameters t_{fc} and t_{wc} represent the thickness of the flange and web respectively, the height of the column is h_c, the width is b_c and the root radio is r_c. The beam profile was the same in all tests. The parameters t_{fb} and t_{wb} denote the thickness of the flange and web respectively, h_c is the height, b_b is the width and r_b the root radio (see Fig. 2).

The material properties were characterized by coupons extracted from the specimens. The beam and column coupons were extracted from the flange of the profiles. Table 4 shows these properties, which will be used to calibrate the finite element models, where f_y and f_u are the yield and ultimate stress, E is Young's module and ε_u is the ultimate strain.

2.1. Instrumentation and load procedure

In all tests, the length of the column L_c was 2010 mm, the distance from the top of the column to the beam L_{cb} was 1030 mm and the load was monotonically applied at a distance of L_b that was recorded in Table 1 (see Fig. 3). No axial force was applied to either the column or the beam. The column was clamped in both sides and the possible lateral-torsional buckling of the beam was avoided by the auxiliary frame structure of the laboratory. In the assembly of the joints, the bolts were hand-tightened to ensure the snug-tight condition.

The tests were instrumented with the aim of obtaining the moment-rotation curves of the column web panel and the joint, and the moment-deformation curves at some key points of the joint.

Thus, to obtain the rotation, three inclinometers were placed as shown in Fig. 3. The inclinometer referenced as IN-1 was in the center of the beam with an offset of 57.5 mm from the end plate. The vertical and horizontal inclinometers placed on the center of the column web panel were designated IN-2 and IN-3, respectively. To evaluate the moment, the load cell (LC-1) measured the load applied to the beam by the hydraulic jack. The displacement sensor (DS-1) was used only to monitor the test process and to confirm the readings of the inclinometers.

To obtain the deformation data, six strain gauges were placed as shown in Fig. 3. Strain gauges G-1 and G-2 were placed on the lower part of the column web panel aligned with the diagonal of the web panel (see break view of Fig. 3) and the strain gauges G-3 to G-6 were placed on the right additional plate, as shown in the detailed view of Fig. 3. G-3 is at the center of the additional plate and aligned with the midpoint of the bolts in tension. G-6 is also at the center of the additional plate and aligned with the bottom flange of the beam. G-4 and G-5 are aligned with the diagonal of the panel and offset 20 mm from the center of the additional plate to avoid interference during the gluing process. The moment-deformation curves were obtained from the data of the strain gauges.

All instrumentation was connected to a data acquisition system model Micro-Measurements System 7000 and measurements were taken every 1 s. Strain gauges Micro-Measurements C2A-06–250LW-120 were used to measure surface deformation. Rotations were measured with one axis inclinometers Pewatron model PEI-S102–1-30-U3–4. The load cell was the Transdutec model CP-2. Finally, the displacement was measured by means of a displacement sensor Vishay Micro-Measurements model CDS-05.

Fig. 4 shows an overview of Test-1 and Test-2 in subfigures (a) and (b), respectively. In Fig. 4(a), the position of inclinometer IN-1 can be observed at the center of the beam near the end plate. On this side of the column web, strain gauges G-1 and G-2 are placed, but in the photo, they are hidden by the additional plate, only the wires are visible. Fig. 4(b) shows the right additional plate with the stain gauges G-3 to G-6. The four gauges in the right additional plate of Test-3 can be seen in Fig. 5(a). Finally, Fig. 5(b) shows the deformation of Test-4 during the loading process and the displacement sensor (DS-1) placed under the beam where the load is applied by the hydraulic jack.

3. Finite element models

3.1. Material, definition of elements and boundary conditions

Four finite element models were performed in Abaqus® Standard

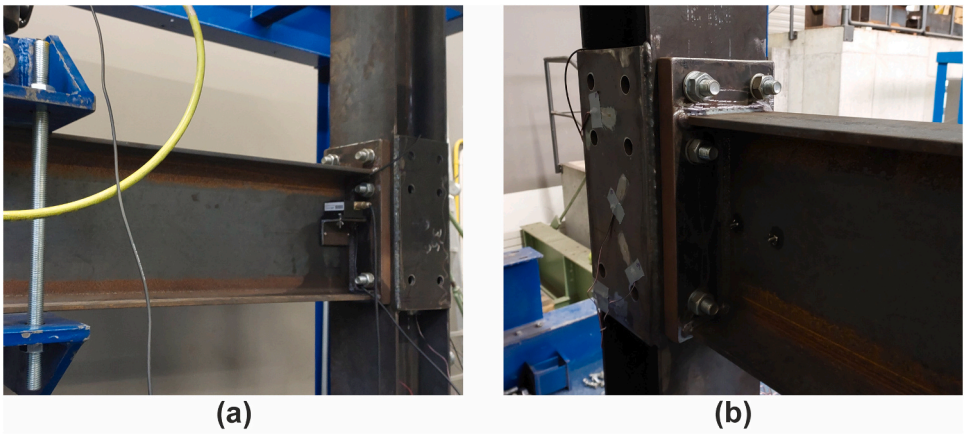

Fig. 4. Joint configuration (a) Test-1 and (b) Test-2.

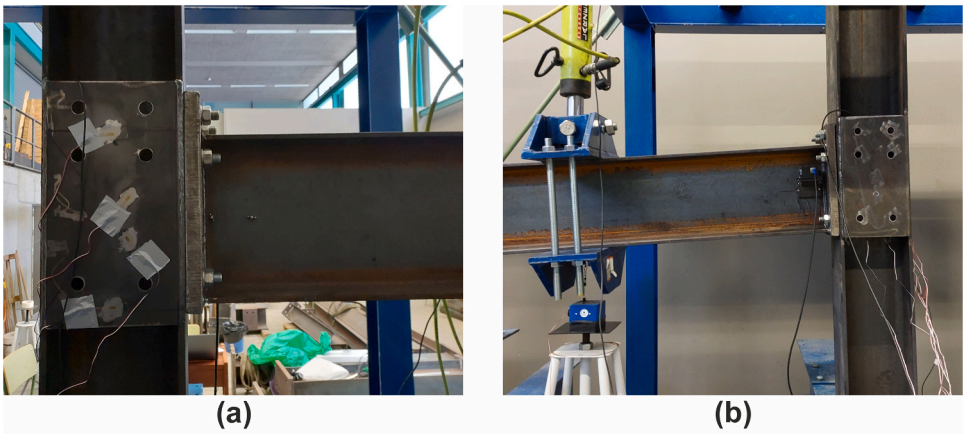

Fig. 5. Joint configuration (a) Test-3 and (b) Test-4.

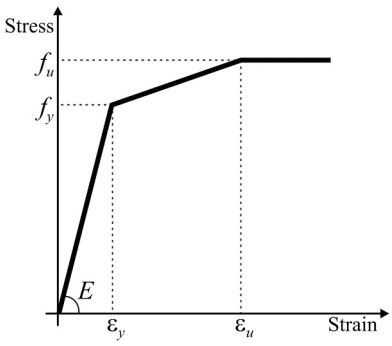

Fig. 6. Stress–strain relationship for steel in the finite element models.

with the same geometric characteristics and boundary conditions as those of the experimental tests described in Section 2. The models take advantage of the symmetry by modelling only half of the specimens. All parts were modeled with 8-nodes solid elements with reduced integration and hourglass control (C3D8R). The parts of the typical model are presented in Fig. 7 with different colors. The model consists of six different parts: beam, column, end plate, additional plate, bolts and the welds between the column and additional plates.

The head, nut and shank of the bolts were modelled together with the washers as a single part. The clearance between the bolt shank and the holes was also considered in the models.

The assumed material properties correspond to the values of Table 4. The quality of the bolts was TR10.9 and they were modelled with the nominal properties of the material. Von Misses criterion was adopted to model the inelastic behavior of the materials by means of a three-linear stress-strain relationship to incorporate strain hardening as shown in Fig. 6. Thus, nonlinearities of the material and geometry were taken into account. To model the loading process, a monotonic displacement was applied to a referent point at the center of the beam tip. This point is the reference of a constraint type rigid body, applied to all nodes of this end section to avoid stress concentrations in the beam. Clamped boundary conditions were applied to the column ends to simulate the experimental test.

Contacts were considered between the following parts: bolts to end plate, end plate to column flange and column flange to bolts. The tangential behavior was modeled with a friction coefficient of 0.25 and the normal behavior with hard contact using the penalty method, which allows the separation after contact. With this method, the contact force is proportional to the penetration distance. The other parts were joined by means of ties: beam to end plate, column flange to additional plate, weld to column flange and weld to additional plate. These ties use the main and secondary surface methodology, constraining the translational degrees and eliminating the degrees of freedom of the secondary surface [18].

3.2. Mesh

The mesh of the models was quite refined and was obtained after a convergence study based on comparative models and previous experience [7,12,13]. In the column, the element size was 5 mm where there

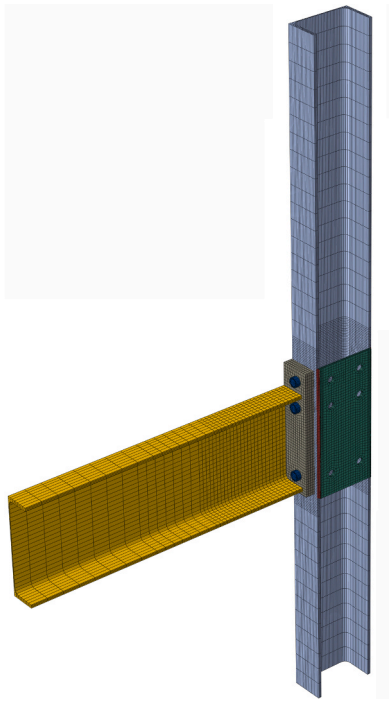

Fig. 7. Parts of the finite element model.

were contacts or large deformations, but 50 mm away from these areas where the deformation was not relevant, thus saving unnecessary computational time. The geometry of all parts has been partitioned to allow structured meshing. Fig. 7 shows the typical mesh of the joint model.

As an example, the model of Test 1 has 54901 elements and 217761 degrees of freedom.

4. Calibration of the finite element models

The finite element models were calibrated using the results from the instrumentation of the experimental tests, that were the moment-rotation and moment-deformation curves, extracted from the data of the load cell, inclinometers and strain gauges.

In the experimental test, the rotation of the joint ϕ_{joint} was obtained by subtracting the rotation of the horizontal inclinometer IN-3 from the rotation of the beam inclinometer IN-1, that is $\phi_{joint} = \phi_{IN-1} - \phi_{IN-3}$. The rotation of the panel was calculated by subtracting the rotation of the inclinometer IN-3 from the rotation of the panel measured by the vertical inclinometer IN-2, that is $\phi_{panel} = \phi_{IN-2} - \phi_{IN-3}$. The moment is the force measured by the load cell LC-1 multiplied by the distance to the flange column, that is $M = F_{LC-1} \cdot L_b$.

In the finite element models, the rotation was obtained from the displacement of two reference points placed at the same position as the inclinometers in the tests.

Fig. 8, Fig. 9, Fig. 10 and Fig. 11 compare the moment-rotation curves of the tests and the finite element models. These comparisons show a very good agreement in both the elastic and plastic range. In Test-3 and Test-4, the column web panel did not reach the plastic range because the tests were stopped to protect the laboratory equipment, due to the load level reached in the tests.

Fig. 12, Fig. 13, Fig. 14 and Fig. 15 compare the moment-deformation curves of the strain gauges of the tests and the finite element models with a reasonable agreement between the results. In all cases, the results show that the lower part of the column web panel, that is the area under compression, was the first area to reach the plastic range in all the tested specimens.

Fig. 16 shows a comparison between the deformation of Test 1 and the corresponding finite element model, where a good match is observed in the deformation pattern in the column flange. Therefore, this similarity and the agreement between the moment-rotation and moment-deformation curves confirm that the finite element model is capable of accurately simulating the joint under investigation.

5. Finite element results and discussion

Fig. 17 shows the von Mises stress and the deformation of the column and the additional plate of the finite element model of the Test-4. The level of load corresponds with the beginning of the plastic range and the scale factor is 20. The stress results of the beam, end plate and bolts have been removed, in order to better display the results. The deformation of the column flange around the bolts is compatible with a circular pattern, a behavior previously described by Loureiro et al. [19]. The force applied to the flange by the bolts produces a bending moment that is transmitted to the additional plate, as shown in the sections S-1 and S-2 of Fig. 17.

The results of the gauges G-3 to G-6 depicted in Fig. 12, Fig. 13, Fig. 14 and Fig. 15 show the behavior of the additional plate. The gauges G-4 are in tension and G-5 in compression (see location in the Fig. 3), showing that the additional plate has a shear deformation. The G-3 and

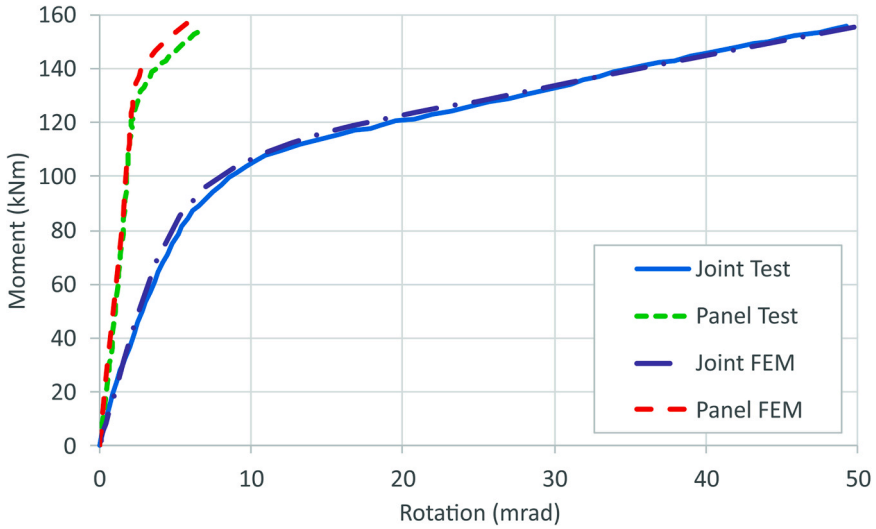

Fig. 8. Moment-rotation curves Test-1.

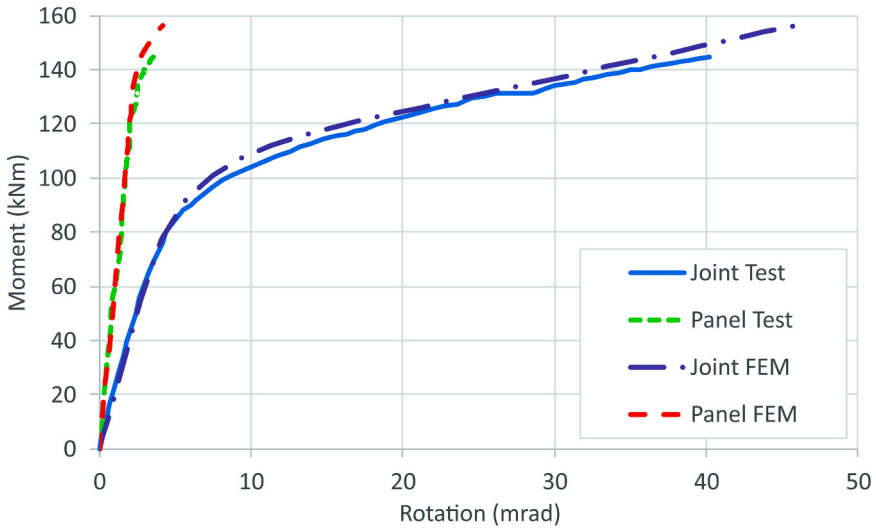

Fig. 9. Moment-rotation curves Test-2.

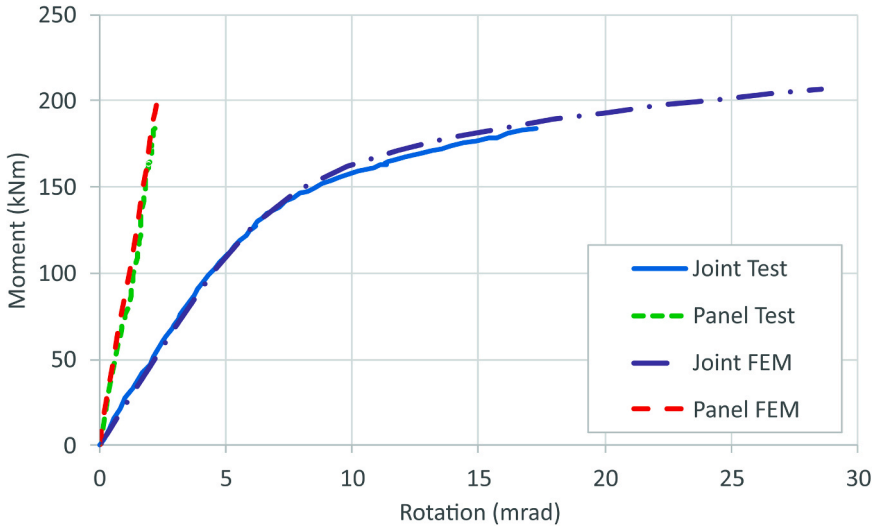

Fig. 10. Moment-rotation curves Test-3.

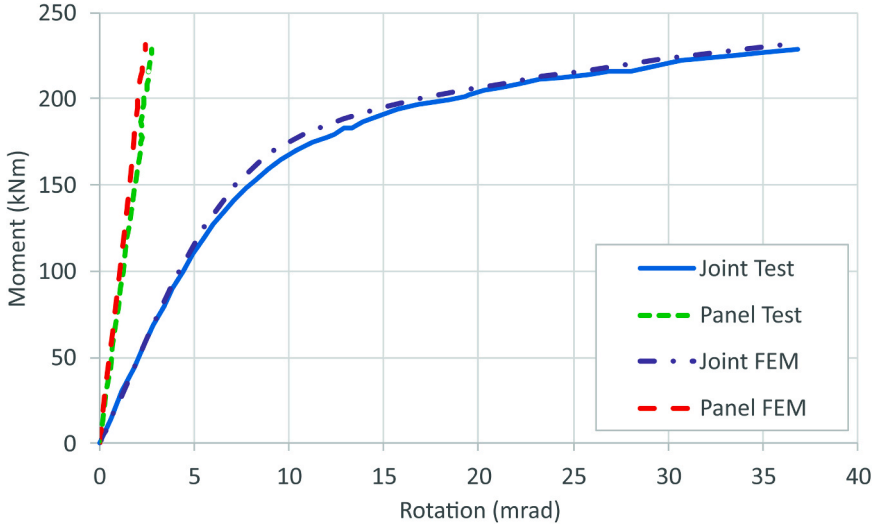

Fig. 11. Moment-rotation curves Test-4.

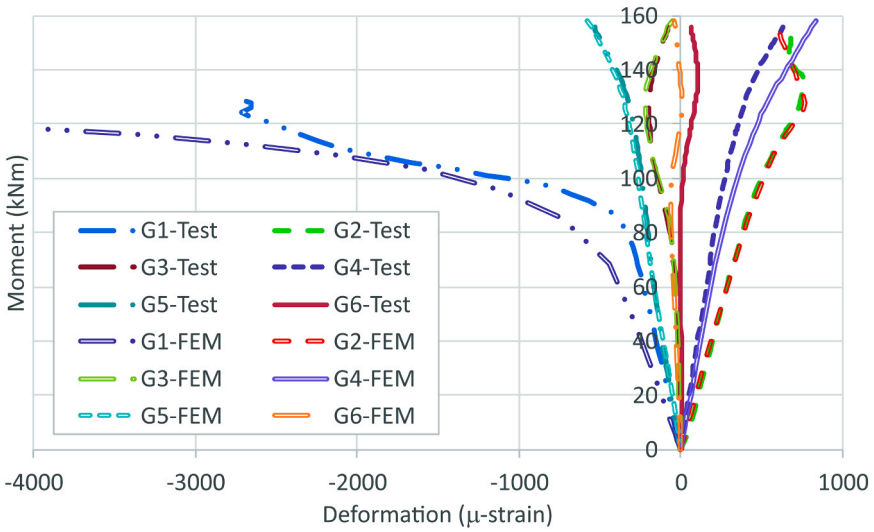

Fig. 12. Moment-deformation curves Test-1.

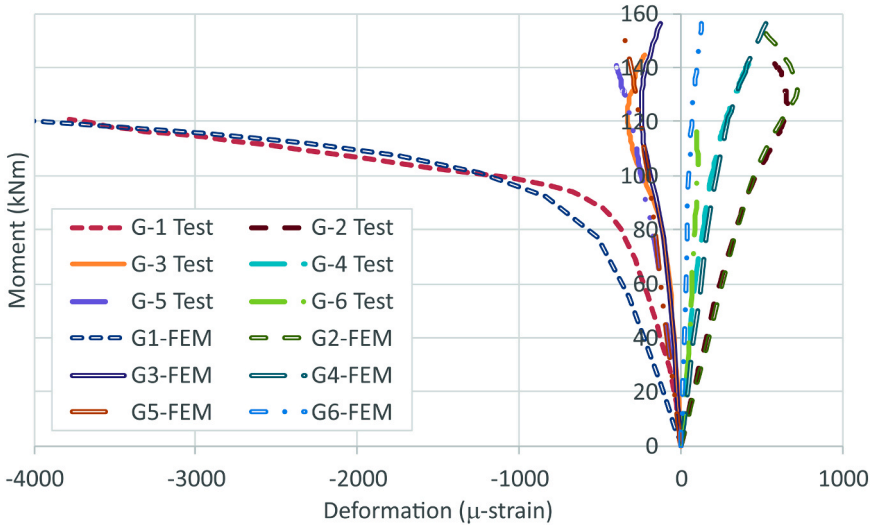

Fig. 13. Moment-deformation curves Test-2.

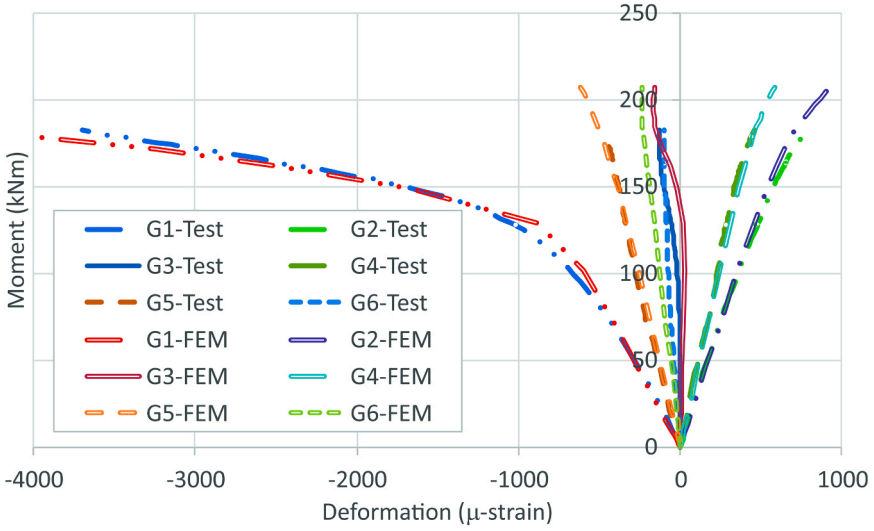

Fig. 14. Moment-deformation curves Test-3.

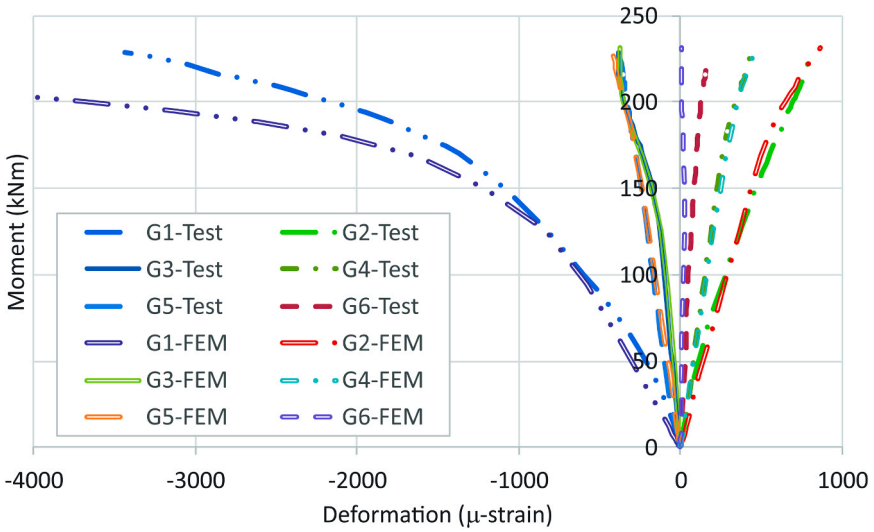

Fig. 15. Moment-deformation curves Test-4.

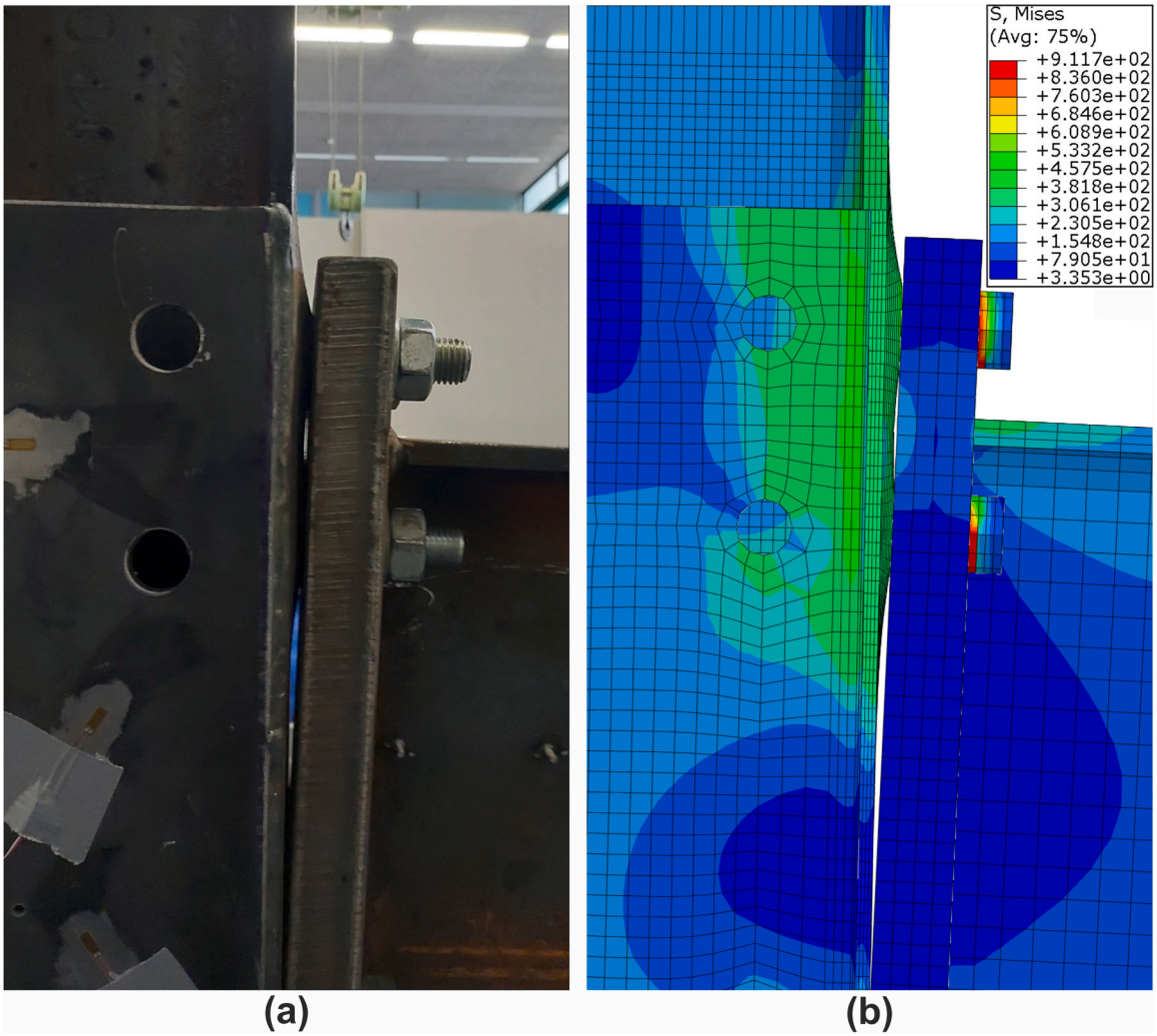

Fig. 16. Deformation comparison between Test-1 and FEM (von Mises stress in MPa).

G-6 gauges were placed in tension and compression zones, respectively; however, they display opposite behavior in the tests with thicker additional plates (Test 2 and Test 4). This effect is due to the bending moment transmitted by the column flange. The section S-1 of Fig. 17 shows the deformation pattern of the additional plate in the tension zone and the section S-2 in the compression zone. It has to be noted that the

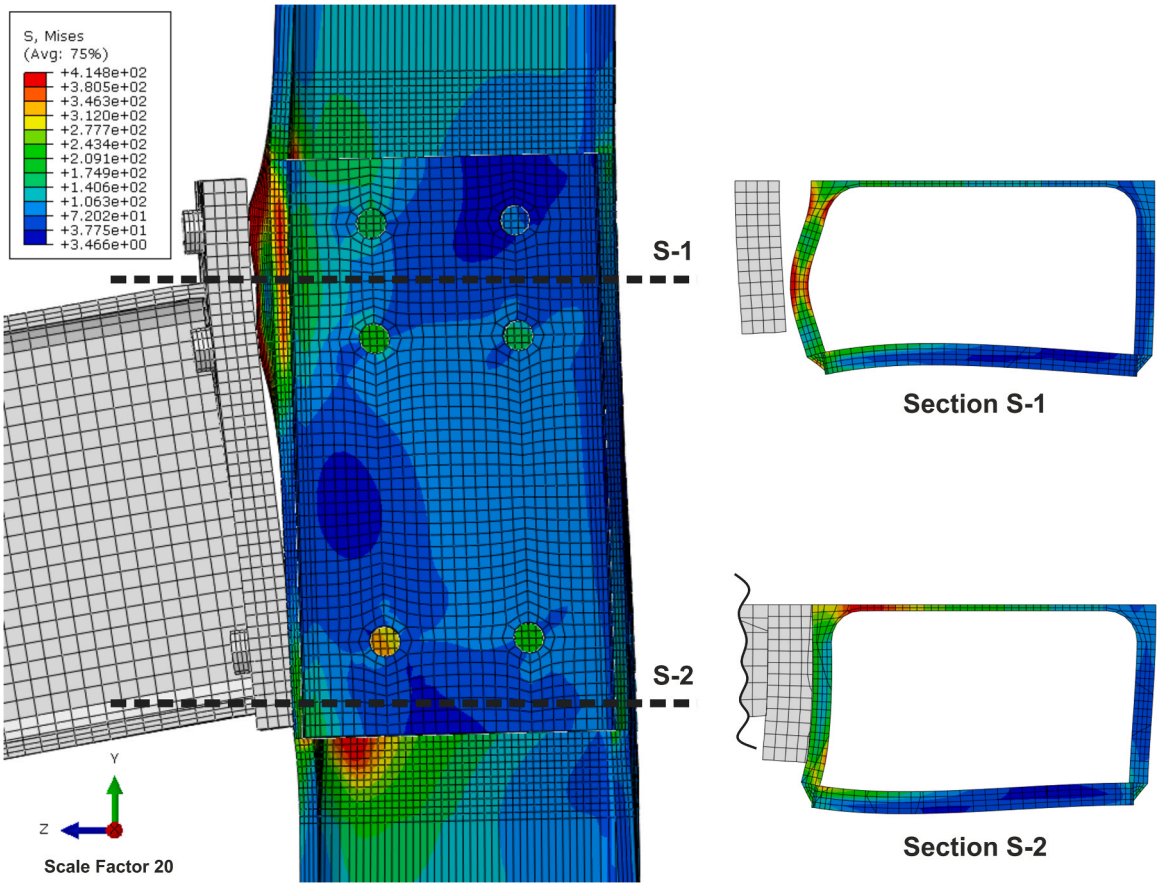

Fig. 17. Stress and deformation of the FEM of the Test-4 (von Mises stress in MPa).

gauges were placed in the external face of the additional plate. On the other hand, in the tests with the thinner plates (Test 1 and Test 3), the G-3 gauges remain with almost no deformation in the elastic range, and in compression in the plastic range. The G-6 gauges are under compression during the loading process.

These results show that the additional plates have a shear deformation, and that the deformation in the tension and compression zones is influenced by the bending moment transmitted by the column flange.

6. Comparison of the finite element models with and without additional plates

In order to evaluate the influence of the additional plates on the shear stress distribution in the column web panel, a comparative study with finite element models was carried out between two configurations, one of them with additional plates and the other one without additional plates. Both models had the same geometric characteristics, namely the column profile type HEA240 and the beam type IPE300. The thickness of the end plate was 15 mm and the horizontal distance between the bolts was 90 mm. In the model with additional plates, the thickness of the additional plates was 10 mm. Fig. 18 shows the shear stress comparison between the finite element models, where subfigures (a) and (b) correspond to the model with and without additional plates, respectively. The illustration in Fig. 18 is a vertical section along the line of the bolts. In both cases the applied moment was 48 kNm. At this load level, the entire joint remained in the elastic range. The pattern of shear stress distribution is similar, but the maximum shear stress is quite different, being 121 N/mm^2 and 98 N/mm^2 for the model with and without additional plates, respectively. It can be concluded that the stiffness of the column web panel in shear with additional plates is approximately 20% higher in the case of this example; therefore, the effect of the additional plates should be considered in the stiffness formulation of the component column web panel in shear.

It should be noted that in Fig. 18 the stress rendering of the bolts, beam and end plate has been removed for a convenient display of the stress in column web.

7. Analytical characterization of the joint stiffness

The type of joint studied is an extended end plate connection with additional plates welded between the column flanges (see Fig. 1). Fig. 19 shows the components of the mechanical model required to calculate its stiffness. This assembly has 6 different components, 4 in each row of bolts and 2 more in the column. The components for each row of bolts are the end plate in bending (epb), the bolts in tension (bt), the column flange in bending (cfb,ap) and the column web in tension (cwt,ap). The other two components in the column are the column web panel in shear (cws,ap) and the column web in compression (cwc,ap).

The components end plate in bending and bolts in tension are defined in Eurocode 3 [3]. But the additional plates modify the behavior of the column components: column flange in bending, column web in tension, column web in compression and column web panel in shear. Stiffness formulations have been proposed by some authors for the first three components. Cabrero et al. [11] have developed a formulation for the column web in tension, column web in compression and column flange in bending. Loureiro et al. [12] have presented a formulation for the stiffness of the column web in tension and the column flange in bending based on the behavior of the E-stub. However, there are no formulations available in the literature for the component column web panel in shear with additional plates welded to the column flanges, so a stiffness formulation is proposed in the following sections of this article.

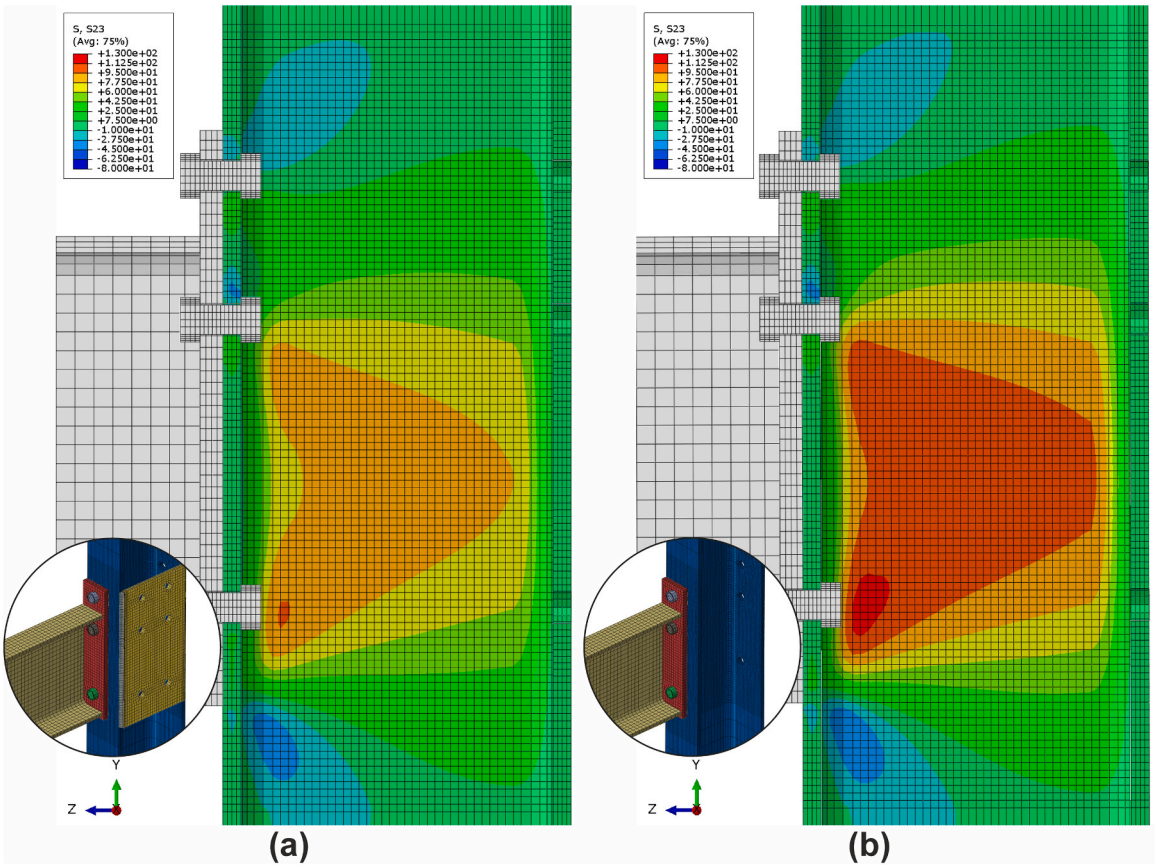

Fig. 18. Shear stress (MPa) in the column web panel. (a) Model with additional plates. (b) Model without additional plates.

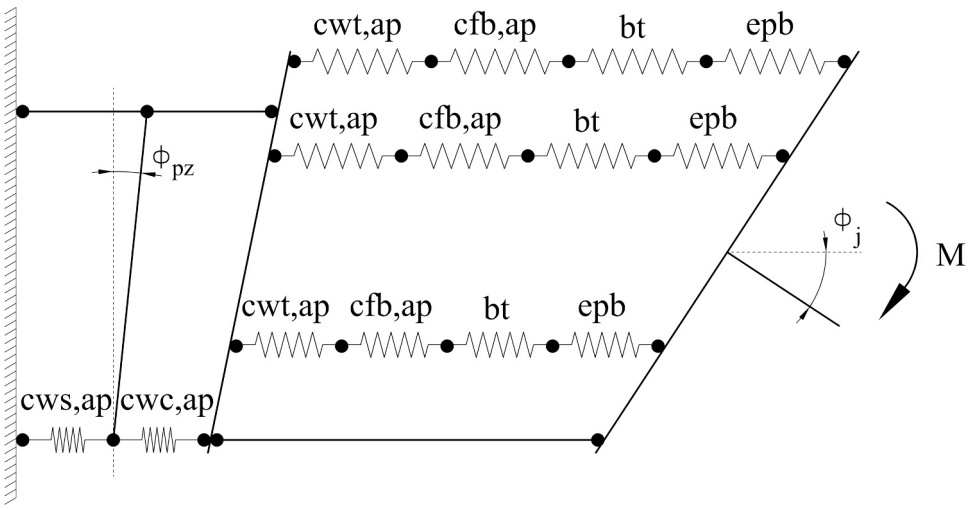

Fig. 19. Mechanical model of the joint.

8. Parametric study with the finite element models

Using the finite element models calibrated with the experimental results (see Sections 3 and 4), an extensive parametric study was conducted. The geometric characteristics of the models are summarized in Table 5. A total of 60 different configurations were analyzed, which were divided into 10 groups with different combinations of the column and beam profiles. The column profile varied from the type HEA 200 to HEB 260 and the beam from the type IPE 270 to IPE 400. Each group had six different configurations by combining two horizontal distances between the bolts (w) and three different thicknesses of the additional plate (t_{ap}). These thicknesses were chosen taking into account the thickness of the column flange, because in building practice they are usually similar; their ratio is in the range of $0.5 \leq t_{ap}/t_{cf} \leq 1.5$.

In all cases, the thickness of the end plate (t_{ep}) was 15 mm, the distance from the top of the end plate to the first row of bolts (e_x) was 30 mm, and the distance from the first row of bolts to the beam flange (m_x) was 40 mm. The distance between the bolt holes in the additional plate (w_{ap}) is equal to w. The remaining geometrical parameters (p_1, p_2, h_{ap}, b_{ep} and h_{ep}) are shown in the last columns of Table 5 and depend on

Table 5
Models of parametric study (dimensions in millimeters).

Group	Column	Beam	w		t_{ap}			h_{ap}	p_1	p_2	b_{ep}	h_{ep}
			w1	w2	$t_{ap}1$	$t_{ap}2$	$t_{ap}3$					
G01	HEA 200	IPE 270	90	100	10	12	15	370	95	160	160	350
G02	HEA 200	IPE 300	90	120	10	12	15	400	95	190	180	380
G03	HEA 240	IPE 300	90	110	10	12	15	400	95	190	170	380
G04	HEA 240	IPE 330	100	120	10	12	15	430	95	220	180	410
G05	HEA 300	IPE 300	100	120	12	15	20	400	95	190	180	380
G06	HEA 300	IPE 400	120	150	12	15	20	500	95	290	210	480
G07	HEB 200	IPE 330	100	120	12	15	20	430	95	220	190	410
G08	HEB 200	IPE 400	100	120	12	15	20	550	95	340	200	530
G09	HEB 260	IPE 450	120	150	12	15	20	550	95	340	210	530
G10	HEB 260	IPE 500	120	150	12	15	20	600	100	380	210	580

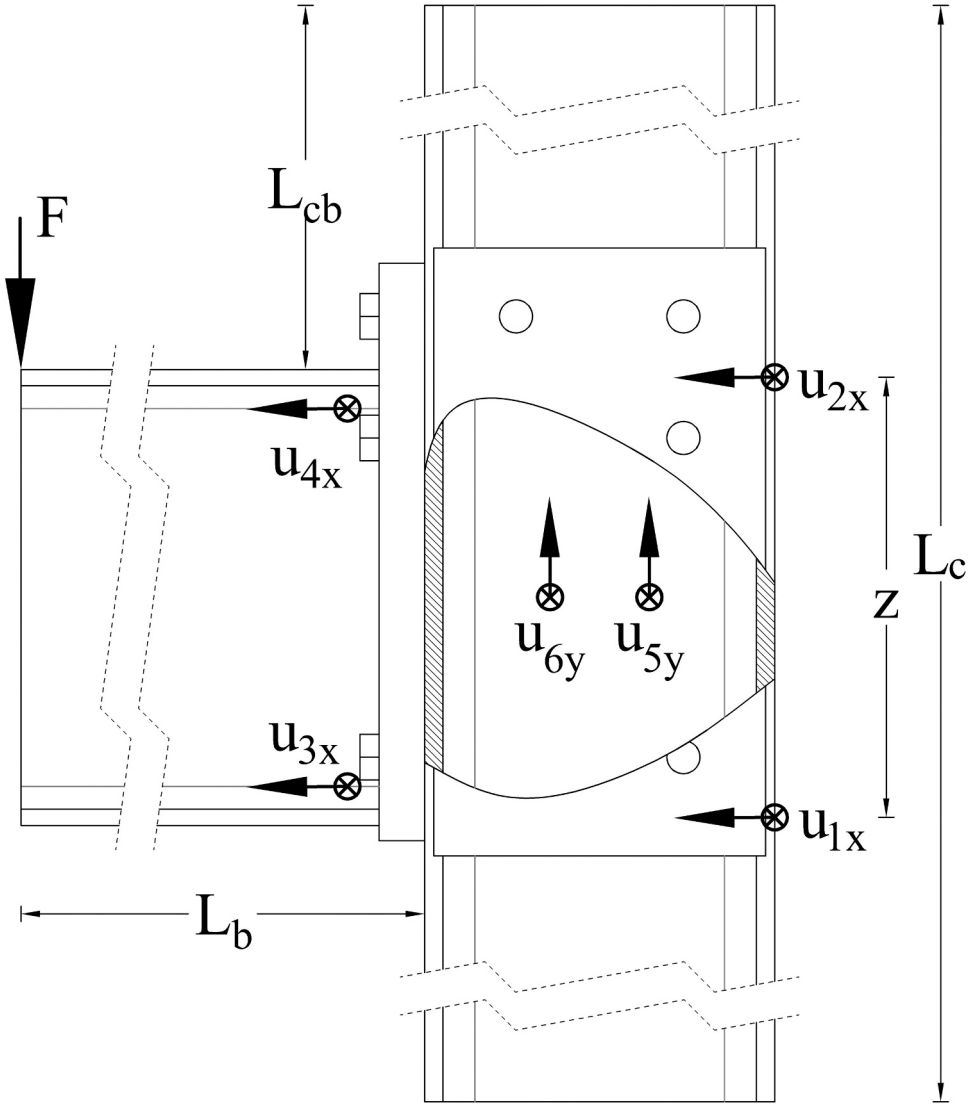

Fig. 20. Reference points in FEM parametric study.

the beam and column profiles. All the parameters were explained graphically in Fig. 2.

Finally, the beam length (L_b) was 3515 mm, the column height (L_c) was 7000 mm, and the distance from the top of the column to the beam (L_{cb}) was 3500 mm (see Fig. 3). These dimensions simulate a typical building size, where the influence of the column shear is less important than in laboratory tests where columns are typically shorter.

8.1. Measurements of moment and rotation in the finite element models

To determine the stiffness of the column web panel in shear and the initial stiffness of the joints, several measurements of rotations and the load were made in the models of the parametric study.

The rotation of the column web panel (ϕ_{pz}) was calculated from the values of the horizontal displacement of two points placed on the column web and represented by u_{2x} and u_{1x} in Fig. 20. The position of these

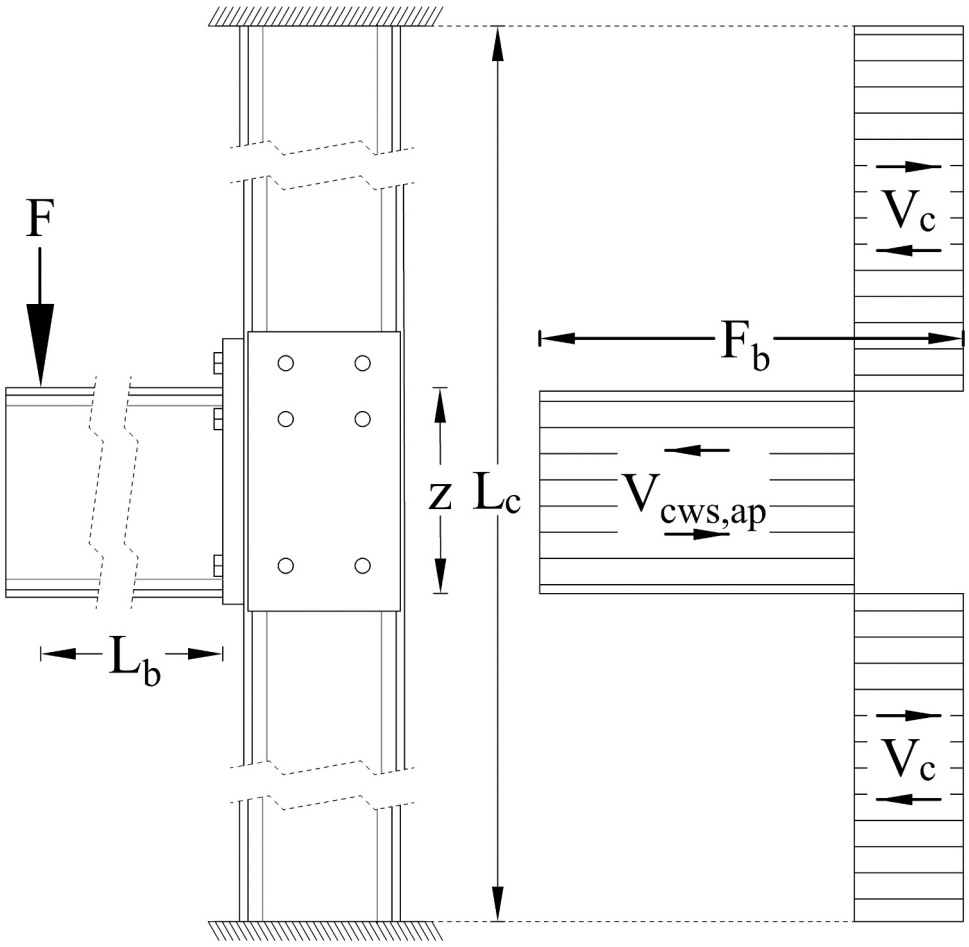

Fig. 21. Shear distribution on the column.

points was chosen to avoid taking into account deformations already considered in other components. In addition, the rotation of the column (ϕ_h) should be subtracted as defined in Eq. 1. Fig. 19 shows the rotation of the column web panel in the mechanical model.

$$\phi_{pz} = \tan^{-1}\left(\frac{u_{2x} - u_{1x}}{z}\right) - \phi_h \tag{1}$$

Where z is the level arm, calculated as the distance from the center of the lower column flange to the middle of the first and second rows of bolts. The rotation of the column (ϕ_h) is defined by Eq. 2.

$$\phi_h = \tan^{-1}\left(\frac{u_{5y} - u_{6y}}{50}\right) \tag{2}$$

The vertical displacements u_{5y} and u_{6y} were measured at the center of the column web panel and the horizontal distance between these points was 50 mm (see break view of Fig. 20).

Eq. 3 evaluates the rotation of the joint (ϕ_j) from the horizontal displacement u_{4x} and u_{3x} of two points at the top and bottom of the flat part of the beam web (see Fig. 20), thus avoiding the shear deformation of the beam. The rotation of the column (ϕ_h) should also be subtracted.

$$\phi_j = \tan^{-1}\left(\frac{u_{4x} - u_{3x}}{d_b}\right) - \phi_h \tag{3}$$

Where d_b is the distance between the points 4 and 3 shown in Fig. 20.

The shear force (F_b) acting in the column is given by the following Eq. 4, where F is the applied force in the beam at a distance L_b from the column flange (see Fig. 21).

$$F_b = \frac{F \bullet L_b}{z} \tag{4}$$

The column of the parametric study was clamped at both ends and the beam was approximately attached in the center of the column, therefore the shear of the column can be defined approximately by the following Eq. 5. Where L_c is the length of the column.

$$V_c \approx \frac{6 \bullet F_b \bullet z}{L_c^3}\left(\frac{L_c}{2}\right)^2 = 1.5 \bullet \frac{z}{L_c} \bullet F_b \tag{5}$$

Eq. 6 defines the parameter ρ that introduces the effect of the column shear.

$$\rho = 1.5 \bullet \frac{z}{L_c} \tag{6}$$

The shear force in the column web panel is the shear force of the joint minus the shear of the column (see Fig. 21).

$$V_{cws,ap} = F_b - V_c = (1 - \rho) \bullet F_b \tag{7}$$

Therefore, the stiffness of the column web panel in shear could be evaluated by Eq. 8, dividing the shear force in the column web panel by the deformation of the web panel.

$$k_{cws,ap,FEM} = 2 \cdot \frac{(1 - \rho) \bullet F_b}{\phi_{pz} \bullet z} \tag{8}$$

The load measured on the finite element model should be multiplied by 2 because the model takes advantage of the symmetry and only half of the joint has been modeled.

Eq. 9 evaluates the initial stiffness of the joint by dividing the applied

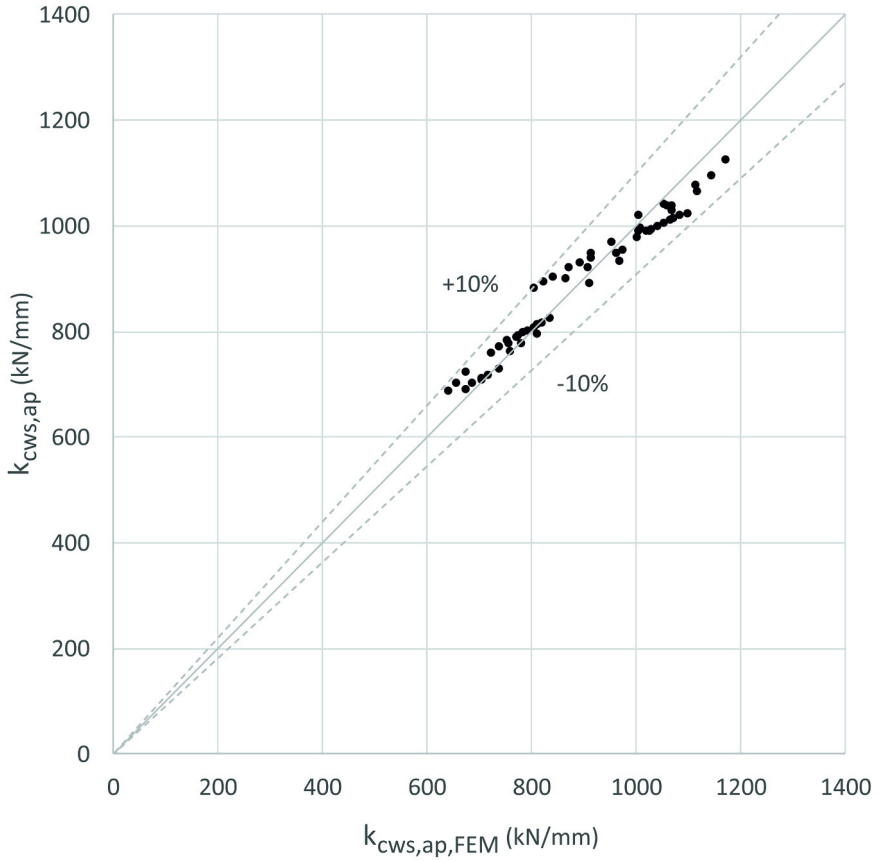

Fig. 22. Stiffness comparison between analytical and finite element models of the component cws,ap.

Table 6
Formulation for joint components.

Component	Stiffness formulation	Parameters	Reference
bt	$\frac{1.6EA_s}{L_{bolt}}$	A_s: tensile stress area of the bolt L_{bolt}: bolt elongation length	Eurocode 3[3]
epb	$\frac{0.9El_{eff}t_{ep}^3}{m^3}$	l_{eff}: the smallest of the effective lengths given for this bolt-row in Table 6.6[3] m: defined in Figure 6.10[3]	
cfb,ap	$2\frac{3EI_{cf}(m+n)^3\left(4\frac{h_c}{2}I_{cf}+I_p(m+n)\right)}{m^3n^2\left(I_pn(m+n)+I_{cf}\frac{h_c}{2}(3m+4n)\right)}$	$I_{cf}=\frac{1}{12}b_{eff}t_{fc}^3$ $I_p=\frac{1}{12}b_{eff}t_{ap}^3$	Loureiro et al.[12]
cwt,ap	$\frac{0.7Eb_{eff}1.5t_{wc}}{d_{wc}}$	$b_{eff}=\frac{b_1(3m+4n)\left(b_1n^3+b_2m\left(m^2+3mn+3n^2\right)\right)}{(m+n)^3(3b_2m+4b_1n)}$ $b_1=d_h+1.2m$ $b_2=d_h+1.2n \quad m=\frac{w}{2}-\frac{t_{wc}}{2}-0.5r_c$ $n=\frac{b_c-w}{2}$ d_h: diameter of the bolt head $d_{wc}=h_c-2\left(t_{fc}+r_c\right)$	
cwc,ap	$\frac{0.7Eb_{eff,cwc}1.25t_{wc}}{d_{wc}}$	$b_{eff,cwc}$: effective width from the article 6.2.6.2[3]	Cabrero et al.[10]
cws,ap	$0.38E\frac{A_{vc}}{z\cdot(1-\rho)}\xi_{cws,ap}$	$A_{vc}=t_{wc}\left(h_c-t_{fc}\right)$ $\xi_{cws,ap}=0.6\left(1+f^{-0.56}\right)$ $f=\frac{t_{fc}n+t_{ap}l_{lib}}{z\sqrt{t_{ap}t_{cf}}}$ with $0.5\le\frac{t_{ap}}{t_{cf}}\le1.5$ $l_{lib}=\left(\frac{b_c}{2}-\frac{b_{co}}{2}\right)\ge0$ $b_{co}=\min(b_b+2t_{ep};\ b_{ep})$ $n=\frac{b_c}{2}-\frac{w}{2}$ $\rho\approx1.5\frac{z}{L_c}$ for clamped columns z: level arm as defined in the article 6.3.3.1 [3]	Section 8.2

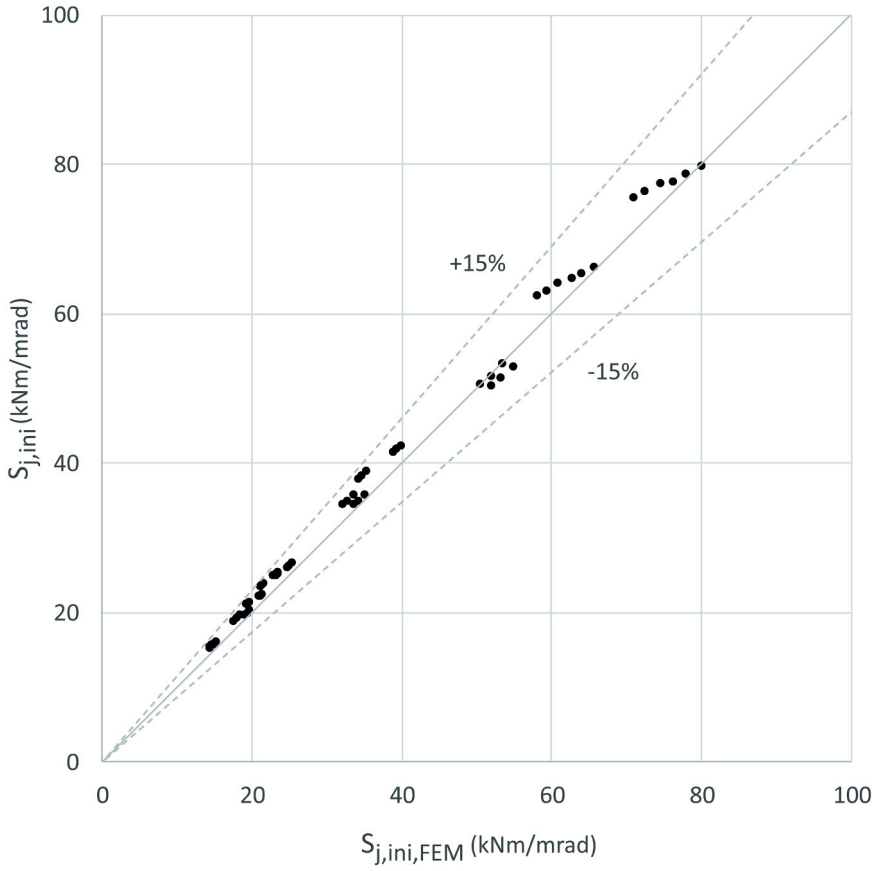

Fig. 23. Initial stiffness comparison between the analytical formulation and the finite element models.

moment by the rotation of the joint.

$$S_{j,ini,FEM} = 2 \cdot \frac{F \cdot L_b}{\phi_j} \tag{9}$$

8.2. Stiffness formulation for the component column web panel in shear with additional plates

The additional plates have a relevant effect on the shear stress of the web panel in the elastic range, as shown in Sections 5 and 6. Therefore, the stiffness formulation for the component column web panel in shear should take these plates into account. Based on this idea, from the results of the parametric study carried out with the calibrated finite element models, a novel formulation for this component is proposed in Eq. 10. The parameter $\xi_{cws.ap}$ introduces the effect of the additional plates in the stiffness of the column web panel in shear.

$$k_{cws,ap} = 0.38 \cdot E \cdot \frac{A_{vc}}{z \cdot (1-\rho)} \cdot \xi_{cws,ap} \tag{10}$$

Where A_{vc} is the shear area of the column defined in Eq. 11 and proposed by Krawinkler et al. [20].

$$A_{vc} = t_{wc} \cdot (h_c - t_{fc}) \tag{11}$$

The parameter $\xi_{cws.ap}$ was obtained by means of regression analysis from the parametric study results and can be evaluated by Eq. 12.

$$\xi_{cws,ap} = 0.6 \cdot \left(1 + f^{-0.56}\right) \tag{12}$$

Where f is a non-dimensional parameter that depends on the geometric characteristics of the joint, as shown in Eq. 13. With a ratio between the thicknesses of $0.5 \leq t_{ap}/t_{cf} \leq 1.5$.

$$f = \frac{t_{fc} \cdot n + t_{ap} \cdot l_{lib}}{z \cdot \sqrt{t_{ap} \cdot t_{cf}}} \tag{13}$$

The length l_{lib} is measured in the compression zone of the column flange, as indicated in Eq. 14.

$$l_{lib} = \left(\frac{b_c}{2} - \frac{b_{co}}{2}\right) \geq 0 \tag{14}$$

Where b_{co} is the minimum value as defined in Eq. 15.

$$b_{co} = \min\left(b_b + 2 \cdot t_{ep}; b_{ep}\right) \tag{15}$$

Finally, Eq. 16 defines the length n.

$$n = \frac{b_c}{2} - \frac{w}{2} \tag{16}$$

The comparison of the analytical stiffness of the column web panel in shear with additional plates, evaluated by Eq. 10, with the stiffness of the finite element models of the parametric study, evaluated by Eq. 8, shows that the mean error is − 0.1%, the standard deviation is 0.039, and the maximum error is 9.3%. These results are shown graphically in Fig. 22 and numerically in the Appendix.

Therefore, the formulation proposed in Eq. 10 is able to evaluate with good accuracy the stiffness of the column web panel in shear when two additional plates are welded between the column flanges.

9. Compilation and validation of the formulation for the initial stiffness of the joint

Table 6 summarizes the formulations required to calculate the initial stiffness of the joint studied, shown in Fig. 1. The mechanical model is shown in Fig. 19 and consists of six components, that have been

identified in Section 7. The sources of these formulations are also reflected in the last column of Table 6, being Eurocode 3 [3], Loureiro et al. [12], Cabrero et al. [10] and Section 8.2 of this article.

In order to validate the initial stiffness formulation presented in Table 6, a comparison was made with the stiffness of the joints of the finite element models of the parametric study obtained from Eq. 9. This comparison is shown graphically in Fig. 23 and numerically in the Appendix. The statistical results show that the mean error was 5.6%, the standard deviation was 0.036, and the maximum error in absolute value was 11.1%. The results show good agreement; therefore, the formulation given in Table 6 is able to evaluate the initial stiffness of the studied joint shown in Fig. 1.

10. Conclusions

The following conclusions can be extracted from the present work:

- An experimental campaign consisting of four tests of extended end plate beam-to-column joints with additional plates welded between column flanges was carried out to obtain load, rotation, and deformation data. From these experimental data, moment-rotation and moment-deformation curves were obtained.
- Finite element models were calibrated against the experimental results by comparing the moment-rotation and moment-deformation curves, showing that they can reproduce with good accuracy the behavior of the joint in the elastic and plastic range.
- An extensive parametric study of 60 different geometries was carried out using the calibrated finite element models.
- A novel analytical formulation was developed for the stiffness of the component column web panel in shear with additional plates welded between column flanges. This formulation was validated with the results of the stiffness of the column web panel with additional plates from the parametric study performed with finite element models.
- By compiling the results of several previous studies, Eurocode 3 and Section 8.2 of this article, all the necessary components to calculate the analytical initial stiffness of the joint were brought together. This analytical initial stiffness was compared with the initial stiffness obtained from the finite element models of the parametric study, resulting in a very satisfactory agreement.

CRediT authorship contribution statement

Jose M Reinosa: Writing – review & editing, Software, Investigation, Conceptualization. **Alfonso Loureiro:** Writing – review & editing, Supervision, Funding acquisition, Conceptualization. **Ruth Gutierrez:** Methodology, Investigation, Formal analysis, Data curation. **Manuel Lopez:** Writing – review & editing, Validation, Methodology, Investigation, Data curation, Conceptualization.

Declaration of Competing Interest

The authors declare that they have no known competing financial interests or personal relationships that could have appeared to influence the work reported in this paper.

Data Availability

Data will be made available on request.

Acknowledgments

The financial support provided through grant PID2020–113895GB-C31 funded by MCIN/AEI/10.13039/501100011033 is gratefully acknowledged.

Appendix

The following table collects the data of the stiffness of the column web panel in shear with additional plates and the initial stiffness of the joint of all models of the parametric study. $k_{cws,ap,FEM}$ and $k_{cws,ap}$ are the stiffness of the web panel in shear of the finite element models of the parametric study and the proposed formulation, respectively. The error between them is $e_{k,cws,ap}$, which is presented in percentage, these numerical values correspond to the data of Fig. 22. $S_{j,ini,FEM}$ and $S_{j,ini}$ are the initial stiffness values of the finite element models of the parametric study and the components method, respectively. The error between them is $e_{S,j,ini}$ which is also expressed in percentage, these numerical values correspond to the data of Fig. 23.

In the next table, the column of the *Ref. Model* is a codification of the geometry of the models of the parametric study defined in Table 5. The first three characters define the group from 01 to 10 (see Table 5). The next character defines the horizontal distance between the bolts (w1 or w2). The last character defines the thickness of the additional plate ($t_{ap}1$, $t_{ap}2$ or $t_{ap}3$). For example, G08,2,3 is a model of the group G08 with a distance between bolts of 120 mm and a thickness of the additional plate of 20 mm.

Ref. Model	$k_{cws,ap,FEM}$ (kN/mm)	$k_{cws,ap}$ (kN/mm)	$e_{k,cws,ap}$	$S_{j,ini,FEM}$ (kNm/mrad)	$S_{j,ini}$ (kNm/mrad)	$e_{S,j,ini}$
G01,1,1	676.3	689.8	2.0%	15.0	15.7	4.6%
G01,1,2	688.1	700.0	1.7%	15.1	15.8	4.5%
G01,1,3	705.3	710.2	0.7%	15.4	16.0	4.3%
G01,2,1	706.4	707.9	0.2%	14.4	15.3	6.5%
G01,2,2	718.7	717.5	-0.2%	14.5	15.5	6.6%
G01,2,3	738.3	726.8	-1.6%	14.8	15.7	6.5%
G02,1,1	640.7	685.5	7.0%	19.1	19.7	2.9%
G02,1,2	656.3	702.1	7.0%	19.6	19.9	1.9%
G02,1,3	673.7	721.2	7.0%	19.7	20.3	2.9%
G02,2,1	760.7	761.1	0.1%	17.7	18.9	6.6%
G02,2,2	780.8	777.5	-0.4%	18.0	19.2	6.8%
G02,2,3	809.7	795.4	-1.8%	18.4	19.7	7.1%
G03,1,1	757.5	777.6	2.7%	21.0	22.1	5.3%
G03,1,2	771.3	787.7	2.1%	21.2	22.3	4.9%
G03,1,3	784.1	797.5	1.7%	21.4	22.4	4.7%
G03,2,1	805.6	805.9	0.0%	19.3	21.1	8.9%
G03,2,2	820.8	814.9	-0.7%	19.5	21.2	8.7%

(*continued on next page*)

(*continued*)

Ref. Model	$k_{cws,ap,FEM}$ (kN/mm)	$k_{cws,ap}$ (kN/mm)	$e_{k,cws,ap}$	$S_{j,ini,FEM}$ (kNm/mrad)	$S_{j,ini}$ (kNm/mrad)	$e_{S,j,ini}$
G03,2,3	835.6	823.1	-1.5%	19.7	21.4	8.6%
G04,1,1	722.1	759.7	5.2%	24.7	26.1	5.4%
G04,1,2	738.4	770.8	4.4%	25.1	26.3	4.9%
G04,1,3	752.2	782.1	4.0%	25.3	26.6	4.8%
G04,2,1	774.0	791.4	2.3%	22.9	24.9	8.6%
G04,2,2	792.6	801.6	1.1%	23.2	25.1	8.1%
G04,2,3	810.6	811.1	0.1%	23.5	25.4	8.0%
G05,1,1	1027.1	988.1	-3.8%	23.3	25.0	7.2%
G05,1,2	1041.5	997.8	-4.2%	23.5	25.1	6.9%
G05,1,3	1052.9	1004.7	-4.6%	23.6	25.2	6.9%
G05,2,1	1065.5	1010.4	-5.2%	21.2	23.5	11.1%
G05,2,2	1083.2	1018.6	-6.0%	21.4	23.7	10.7%
G05,2,3	1098.4	1023.2	-6.8%	21.6	23.9	10.7%
G06,1,1	805.3	879.9	9.3%	38.9	41.4	6.5%
G06,1,2	822.9	892.4	8.5%	39.4	41.8	6.0%
G06,1,3	840.2	903.4	7.5%	39.9	42.3	5.8%
G06,2,1	870.9	920.4	5.7%	34.3	37.8	10.1%
G06,2,2	892.6	930.6	4.3%	34.8	38.2	9.8%
G06,2,3	915.4	938.0	2.5%	35.4	38.9	9.9%
G07,1,1	973.9	953.1	-2.1%	33.6	34.4	2.3%
G07,1,2	1021.6	989.7	-3.1%	34.4	35.0	1.8%
G07,1,3	1068.8	1037.2	-3.0%	35.1	35.8	1.9%
G07,2,1	1058.8	1036.2	-2.1%	32.1	34.4	7.0%
G07,2,2	1114.0	1075.3	-3.5%	32.9	35.0	6.5%
G07,2,3	1172.0	1125.3	-4.0%	33.6	35.8	6.5%
G08,1,1	911.9	889.8	-2.4%	51.9	50.2	-3.3%
G08,1,2	968.5	932.6	-3.7%	53.4	51.3	-3.9%
G08,1,3	1029.2	992.0	-3.6%	54.9	52.8	-3.9%
G08,2,1	1001.5	978.3	-2.3%	50.5	50.5	0.0%
G08,2,2	1068.6	1026.8	-3.9%	52.0	51.6	-0.7%
G08,2,3	1143.3	1094.0	-4.3%	53.6	53.2	-0.7%
G09,1,1	914.6	945.8	3.4%	62.8	64.7	2.9%
G09,1,2	954.6	969.4	1.6%	64.0	65.4	2.1%
G09,1,3	1007.3	995.8	-1.1%	65.6	66.2	0.9%
G09,2,1	1005.3	1018.5	1.3%	58.2	62.5	7.3%
G09,2,2	1052.8	1040.7	-1.1%	59.3	63.1	6.3%
G09,2,3	1117.6	1063.8	-4.8%	60.9	64.0	5.1%
G10,1,1	865.3	898.5	3.8%	76.3	77.7	1.9%
G10,1,2	907.6	921.3	1.5%	77.9	78.6	0.9%
G10,1,3	963.6	946.9	-1.7%	80.0	79.7	-0.4%
G10,2,1	953.6	968.8	1.6%	71.0	75.5	6.4%
G10,2,2	1003.8	990.2	-1.4%	72.5	76.3	5.2%
G10,2,3	1072.6	1012.6	-5.6%	74.6	77.4	3.8%

References

[1] Faella C, Piluso V, Rizzano G. Structural steel semirigid joints. Boca Ratón, Florida: CRC Press LLC; 2000.

[2] Celik HK, Sakar G. Semi-Rigid connections in steel structures: State-of-the-Art report on modelling, analysis and design. Steel Compos Struct 2022;45-1:1–21. https://doi.org/10.12989/scs.2022.45.1.001.

[3] EUROCODE 3, Design of Steel Structures – part 1.8: Design of joints CEN, Brussels, 2005.

[4] Jaspart J.P. Etude de la semi-rigidité des noeuds poutre-colonne et son influence sur la résistance et la stabilité des ossatures en acier. PhD thesis. Belgium: University of Liege; 1991.

[5] Lima LRO, Simões da Silva L, Vellasco PCG, Andrade SAL. Experimental evaluation of extended endplate beam-to-column joints subjected to bending and axial force. Eng Struct 2004;26(10):1333–47. https://doi.org/10.1016/j.engstruct.2004.04.003.

[6] Lemonis ME, Gantes CJ. Mechanical modeling of the nonlinear response of beam-to-column joints. J Constr Steel Res 2009;65(4):879–90. https://doi.org/10.1016/j.jcsr.2008.11.007.

[7] Lopez M, Loureiro A, Gutierrez RM, Reinosa JM. A new analytical formulation for the stiffness and resistance of the additional plate in bending in beam-to-beam steel joints. Eng Struct 2021;228:111476. https://doi.org/10.1016/j.engstruct.2020.111476.

[8] Daniūnas A, Urbonas K. Analysis of the steel frames with the semi-rigid beam-to-beam and beam-to-column knee joints under bending and axial forces. Eng Struct 2008;30(11):3114–8. https://doi.org/10.1016/j.engstruct.2008.04.027.

[9] De Lima LRO, De Andrade SAL, da S, Vellasco PCG, da Silva LS. Experimental and Mechanical Model for Predicting the Behaviour of Minor Axis Beam-to-column Semi-rigid Joints. Int J Mech Sci 2002;44(6):1047–65. https://doi.org/10.1016/S0020-7403(02)00013-9.

[10] Costa R, Valdez J, Oliveira S, Simões da Silva L, Bayo E. Experimental behaviour of 3D end-plate beam-to-column bolted steel joints. Eng Struct 2019;188:277–89. https://doi.org/10.1016/j.engstruct.2019.03.017.

[11] Cabrero JM, Bayo E. The semi-rigid behaviour of three-dimensional steel beam-to column joints subjected to proportional loading. Part II: theoretical model and validation. J Constr Steel Res 2007;63(9):1254–67. https://doi.org/10.1016/j.jcsr.2006.11.005.

[12] Loureiro A, López M, Gutiérrez R, Reinosa JM. Experimental and numerical analysis of E-stubs in three dimensional joints: a new analytical formulation for the stiffness calculation. Eng Struct 2013;53:1–9. https://doi.org/10.1016/j.engstruct.2013.03.035.

[13] Bayo E, Loureiro A, Lopez M, Simões da Silva L. General component based cruciform finite elements to model 2D steel joints with beams of equal and different depths. Eng Struct 2017;152:698–708. https://doi.org/10.1016/j.engstruct.2017.09.042.

[14] Corman A, Demonceau JF, Jaspart JP. Analytical model for the panel zone resistance in welded steel beam-to-column joints. J Constr Steel Res 2022;189:107099. https://doi.org/10.1016/j.jcsr.2021.107099.

[15] Golea T, Corman A, Mathieu J, Duchêne Y, Jaspart JP, Demonceau JF. An innovative mechanical model for structural steel joints. Eng Struct 2023;277:115459. https://doi.org/10.1016/j.engstruct.2022.115459.

[16] Lopez M, Loureiro A, Bayo E. Shear behaviour of trapezoidal column panels. II: parametric study and cruciform element. J Constr Steel Res 2015;108:70–81. https://doi.org/10.1016/j.jcsr.2014.10.029.

[17] Augusto H, Simões da Silva L, Rebelo C, Castro JM. Characterization of web panel components in double-extended bolted end-plate steel joints. J Constr Steel Res 2016;116:271–93. https://doi.org/10.1016/j.jcsr.2015.08.022.

[18] ABAQUS documentation analysis user's manual, Version 6.17
[19] Loureiro A, López M, Gutiérrez R, Reinosa JM. A new analytical formulation for the E-stub strength calculation in three dimensional steel joints with additional plates welded to the weak axis. Eng Struct 2013;56:2263–72. https://doi.org/10.1016/j.engstruct.2013.08.037.
[20] Krawinkler H, Bertero VV, Popov EP. Shear behaviour of steel frame joints. J Struct Div ASCE 1975;101(11):2317–36.